J Therm Anal Calorim (2012) 108:1079–1084
DOI 10.1007/s10973-011-1966-y

Nanocrystalline TiO_2/SnO_2 composites for gas sensors

M. Radecka · A. Kusior · A. Lacz · A. Trenczek-Zajac · B. Lyson-Sypien · K. Zakrzewska

ICVMTT2011 Conference Special Chapter

Abstract TiO_2/SnO_2 nanocomposites are studied as potential candidates for gas sensors. Commercial metal oxide nanopowders milled for 1 h in ethanol are used for preparing nanocomposites with varied composition from 100 mol% TiO_2 to 100 mol% SnO_2. Brunauer–Emmett–Teller (BET) adsorption isotherms served to determine specific surface area, SSA. The particle size distribution is established by means of Dynamic Light Scattering, DLS technique. Differential Thermal Analysis and Thermogravimetry, DTA/TG measurements within the temperature range of 20–900 °C indicate better stability of nanomaterials composed of bigger particles or agglomerates. The total mass loss varies from 0.9 to 8.5% for 100 mol% SnO_2 and 100 mol% TiO_2, respectively. The only gaseous products of decomposition are water and carbon dioxide. X-ray diffraction analysis of nanocomposites indicates two separate phases of different crystallite size, i.e., smaller rutile TiO_2 (9 nm) and larger cassiterite SnO_2 (28 nm). Gas sensor dynamic responses at 400 °C to the reducing gas—ammonia (NH_3) are detected in the concentration range extending from 100 ppm to −5000 ppm. Nanosensor of 50 mol% SnO_2/50 mol% TiO_2 is stable and sensitive to the interaction with NH_3 and gives the highest response at 400 °C.

M. Radecka (✉) · A. Kusior · A. Lacz · A. Trenczek-Zajac
Faculty of Materials Science and Ceramics, AGH University of Science and Technology, al. A. Mickiewicza 30, 30-059 Krakow, Poland
e-mail: radecka@agh.edu.pl

B. Lyson-Sypien · K. Zakrzewska
Faculty of Electrical Engineering, Automatics, Computer Science and Electronics, AGH University of Science and Technology, al. A. Mickiewicza 30, 30-059 Krakow, Poland

Keywords TiO_2 · SnO_2 · Gas sensors · Nanopowders · Composites · Differential thermal analysis · Thermogravimetry · Mass spectrometry

Introduction

Metal oxides, such as TiO_2, SnO_2, ZnO, WO_3, and Fe_2O_3, are well known for their remarkable ability to change the electrical resistivity in response to oxidizing and reducing gases. Gas sensing properties of these materials are determined by the surface states and morphology of the metal oxides. Nanomaterials and nanostructures, such as nanowires, nanotubes and nanodots, seem to be particularly interesting for this purpose because of the increased surface-to-volume ratio. Reduced dimensionality of nanosensors affects the efficiency of gas adsorption process and improves sensitivity of nanomaterials [1]. However, there are additional basic features, namely quantum confinement, nanoparticle morphology and aggregation as well as nanomaterial agglomeration [2] that play an important role in decreasing operating temperature and improving sensor selectivity.

Detection of ammonia (NH_3), gas, extremely dangerous to human health, constitutes a challenge for environmental, automotive and chemical industry as well as the medical diagnostics [3]. In order to implement the resistive type sensors in these four major areas, different demanding requirements as to the detection limit, response time and temperature range are formulated [3].

However, most of the semiconductor gas sensors exhibit very small changes in the electrical resistance upon exposure to NH_3 hence very low NH_3 sensitivity. It is generally accepted that the reducing gases to be detected remove some of the adsorbed oxygen thus change the overall

conductivity and create the sensor signal. The following competitive reactions can occur in the presence of ammonia and oxygen [4, 5]:

$$2NH_3 + 7O^-_{(ad)} \rightarrow 2NO_2 + 3H_2O + 7e^-,$$

$$2NH_3 + NO_2 + O^-_{(ad)} \rightarrow 3/2N_2 + 3H_2O + 1e^-$$

Interference from NO_x and NO_2 in particular, being an oxidation product of NH_3, is considered to be one of the reasons for the observed low NH_3 sensitivity. Efforts have been made to improve the selectivity and enhance the sensitivity towards ammonia. Selective metal-oxide gas sensors can be obtained by doping or using catalysts that enhance the chemisorption of specific gases or by creating nanocomposites of different metal oxides.

Recently, one can observe a growing interest in the composite materials that consist of two metal oxides, e.g., SnO_2–ZnO [6–8], Fe_2O_3–ZnO [9], Fe_2O_3–SnO_2 [10, 11], WO_3–SnO_2 [12], SnO_2–TiO_2 [13] as well as three components like SnO_2–TiO_2–In_2O_3 [14, 15] for gas sensor applications. It has been proved that coupled systems increase the gas sensor response [12, 14], sensitivity and selectivity towards detected gas [6, 9, 14]. Moreover, this enables to lower the operating temperature [13] and improves thermal stability of the gas sensor [6].

Among many possible metal oxide systems for gas detection, special attention has been paid to solid solutions and composites of TiO_2–SnO_2 [13, 17–20]. Nowadays, tin and titanium dioxides are under investigation particularly in a nanocrystalline form.

The aim of this work has been to study TiO_2/SnO_2 system based on commercial nanopowders. The effect of composition of nanocrystalline TiO_2/SnO_2 mixtures on the sensor dynamic responses to NH_3 has been demonstrated. Material characterization is important for predicting the best performance of composite nanosensors. Special importance is paid to Differential Thermal Analysis (DTA), Thermogravimetry (TG) and Mass Spectrometry (MS) as suitable methods for evaluation of this type of powders [21–25]. Moreover, application of these methods is necessary prior to further processing of nanopowders for gas sensing purposes. DTA/TG and mass spectrometry allow us to determine suitable thermal conditions of the sensor preparation and operation.

Experimental

Commercial rutile–TiO_2 (purity 99.5%) and SnO_2 (purity non-specified) nanopowders from Sigma-Aldrich were used to prepare the composites. Appropriate amounts of metal oxides were mixed by milling with zirconia balls in ethanol for 1 h. Composition of the prepared composites of TiO_2/SnO_2 was varied from 100 mol% TiO_2 to 100 mol% SnO_2.

Specific surface area, SSA, of nanopowders was determined from nitrogen adsorption BET (Brunauer–Emmett–Teller) isotherms obtained with ASAP 2010 Chemi System Micromeritics Instruments.

The particle size distribution of pure TiO_2 and SnO_2 nanopowders dissolved in water and ethanol was established on the basis of the Brownian motion using Dynamic Light Scattering technique, DLS with a Nanosizer-ZS, Malvern Instruments.

Differential Thermal Analysis and Thermogravimetry, DTA/TG, measurements were carried out on a SDT 2960 TA Instruments apparatus in the temperature range of 20–900 °C. The nanopowder samples of mass around 20 mg were placed in standard platinum crucibles and heated at a rate of 10 °C min^{-1}. The measurements were carried out under dynamic conditions in the synthetic air atmospheres (<15 ppm H_2O) under a flow of 100 cm^3 min^{-1}. Volatile products of decomposition were analyzed by a quadrupole mass spectrometer (ThermoStar QMS 300 Balzers) connected on-line to the SDT 2960 system by a quartz capillary heated up to 200 °C.

Nanosensors were prepared in a form of circular tablets calcined from the nanopowders at a pressure of 25 MPa and temperature of 400 °C. The temperature of calcination was established on the basis of DTA/TG and MS measurements.

Crystallographic properties of the both nanopowders and sensing tablets were determined by X-ray diffraction using an X'Pert MPD Philips diffractometer in a Bragg–Brentano geometry.

Gas sensor dynamic responses defined as $S = (R - R_o)/R_o$ where R is the electrical resistance upon gas introduction and R_o is the electrical resistance in air as a reference gas were recorded in a system described in detail in [16]. The responses to the reducing gas NH_3 were detected at a constant temperature of 400 °C upon changing concentration of ammonia within the range of 100–5000 pm. Ammonia was mixed with air by adjusting the corresponding flow rates. The total flow of NH_3 + air mixture was kept constant at 60 sccm.

Results and discussion

Chemical composition, SSA, and the crystallite size D of the starting materials and prepared nanocrystalline TiO_2/SnO_2 composites are given in Table 1.

Figure 1 demonstrates distribution of the particle size for the commercial nanopowders of the starting materials, i.e., pure rutile TiO_2 (a) and SnO_2 (b). As compared with the crystallite size obtained from the studies of X-ray

Table 1 Chemical composition, specific surface area, SSA as well as the crystallite diameter D of the starting materials and prepared nanocrystalline TiO_2/SnO_2

Chemical composition mol % TiO_2	Specific surface area SSA/m^2 g^{-1}	D from XRD/nm	
		SnO_2	TiO_2
0	21.2	28	
2	23.2	28	
10	26.9	28	
20	34.7	28	
50	64.5	26	11
80	115.3	28	11
90	137.1	21	9
95	146.3		9
100	158.5		8

diffraction (see Table 1) high degree of agglomeration can be seen. However, SnO_2 nanopowder forms larger agglomerates (80–300 nm in diameter) on the average than TiO_2 (40–100 nm).

As it can be concluded from the results presented in Table 1, and in Fig. 1, the grain sizes of commercial nanopowders of the starting materials, i.e., pure rutile TiO_2 and SnO_2 are not well matched. The crystallite size is much lower in the case of TiO_2 than that of SnO_2. This has profound consequences for morphology of TiO_2/SnO_2 composites as well as for their gas sensing performance.

As shown by DTA/TG and MS measurements, the results of which are presented in Figs. 2 and 3, the material with smaller grain size is less stable than the one of larger grains. The loss of mass upon heating is more pronounced for TiO_2 than for SnO_2. Mass spectra for SnO_2 are not presented here because the signals are weak and noisy.

Thermal decomposition of nanopowders proceeds through overlapping stages. The total mass loss depends on the composition of materials and varies from 0.9% for 100 mol % SnO_2 to 8.5% for 100 mol % TiO_2 (Fig. 2). The mass spectrum of the gas produced by decomposition of TiO_2/SnO_2 composites contains the following m/z signals: 12, 17, 18 and 44, where m is a mass while z is a charge of the molecule in electron charge units. This leads to a conclusion that the only gaseous products of decomposition are water and carbon dioxide. The mass spectrum for these compounds taken from the NIST database [26] is as follows: H_2O—16(0.9), 17(21), 18(100) and CO_2—12(8.7), 16(9.6), 28(9.8), 44(100), where the first number is the m/z value, the number in the brackets complies with an intensity. The signals for m/z equal to 16 and 28 cannot be taken into account as the measurements are performed in air containing oxygen and nitrogen. For the nanometric titanium and tin oxides and

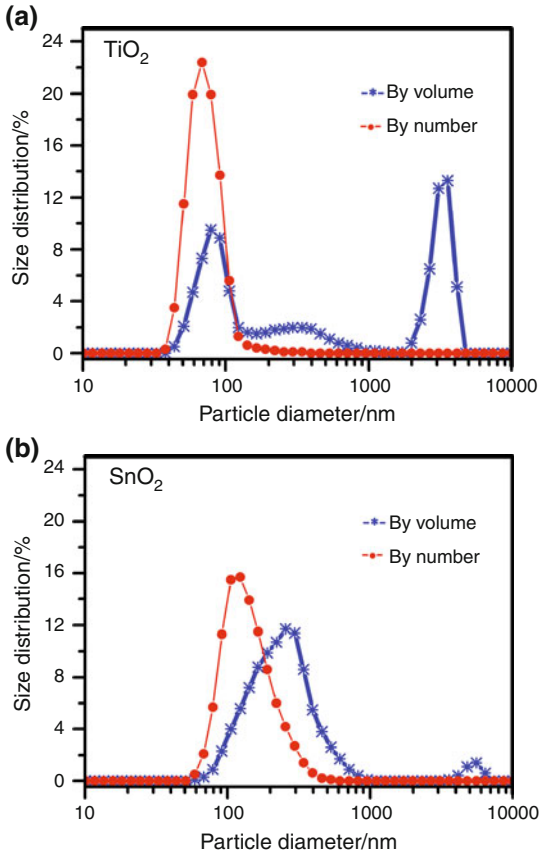

Fig. 1 Distribution of particle diameter for commercial nanopowders of the starting materials, i.e., pure rutile TiO_2 (**a**) and SnO_2 (**b**) obtained from dynamic light scattering, DLS

their composites, the mass loss starts at about 45 °C. This first step of decomposition occurs between 45 and 180 °C and is described by a small endothermic effect on the DTA curve. Analysis of the mass spectrum of the gaseous products accompanying decomposition of the material indicates the presence of water, only ($m/z = 18$ on the ion current line) in the analyzed temperature range (Fig. 3). Therefore, it can be stated that this step is a result of dehydratation—removing water absorbed by the materials. For the analyzed samples, starting from the temperature of about 180 °C, strong exothermic effects on DTA curves together with a large amount of CO_2 evolved ($m/z = 44$) and H_2O ($m/z = 18$) are observed (Fig. 3). All this strongly indicates the combustion process of some organic residue resulting probably from the nanopowders synthesis, distinctly seen for bulk TiO_2, and its composites with high fraction of TiO_2 the more so as, the mass loss for these materials is significant.

Figure 4 shows the comparison between X-ray diffraction patterns of nanopowders and calcined tablets of pure, starting TiO_2 and SnO_2 commercial materials. As it can be seen, apparently there is no big difference between XRD

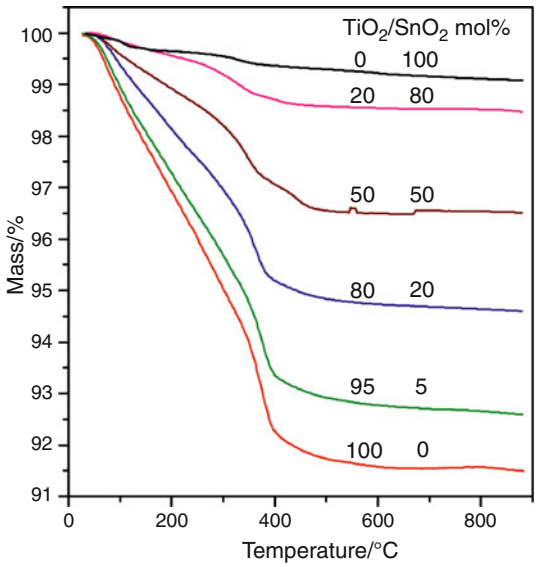

Fig. 2 Mass loss determined from the thermogravimetric (TG) measurements as a function of temperature for nanopowders of TiO_2/SnO_2

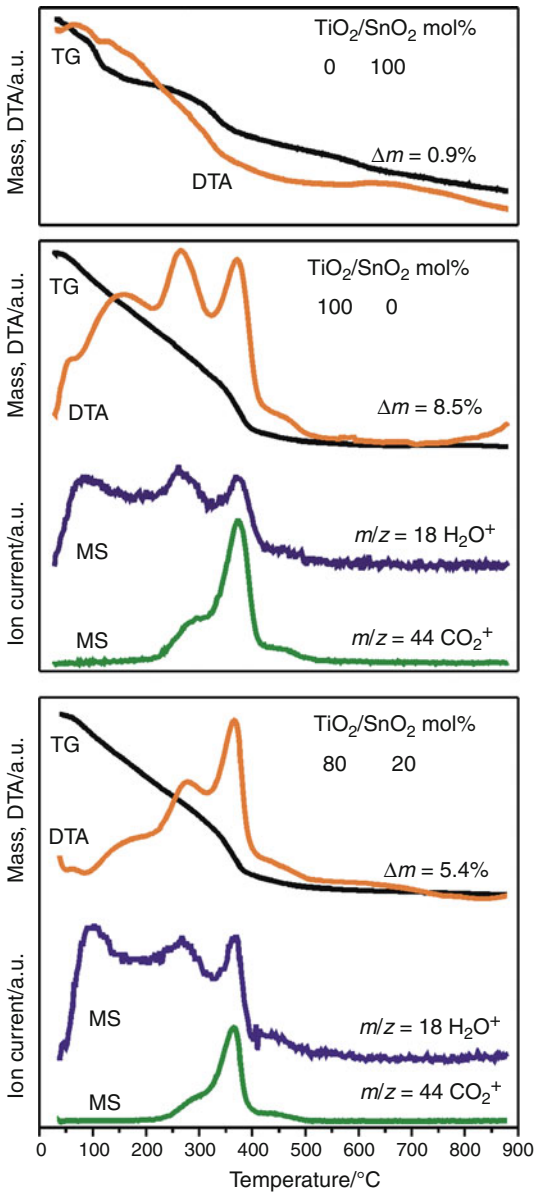

Fig. 3 Simultaneous TG/DTA and mass spectroscopic (MS) curves as a function of temperature for nanopowders of TiO_2/SnO_2

patterns of the nanopowders and tablets. This indicates that the calcination temperature of 400 °C is low enough to inhibit the growth of nanoparticles.

Figure 5 demonstrates the evolution of the crystallographic structure as determined from X-ray diffraction upon changes in the composition of TiO_2/SnO_2 nanopowder mixtures. Two separate phases of different crystallite sizes, that of smaller rutile TiO_2 and that of larger cassiterite SnO_2 can be easily distinguished. TiO_2 rutile XRD peaks are wide as compared with those of SnO_2. Mixing of both nanopowders results in TiO_2/SnO_2 composites of small TiO_2 and large SnO_2 grains. Because of smaller molecular weight of TiO_2 (79 g mol^{-1}) as compared to that of SnO_2 (150 g mol^{-1}) combined with fine grains of TiO_2, the X-ray diffraction peaks from this phase cannot be observed until the composition of the mixture reaches 50 mol% SnO_2/50 mol% TiO_2. The crystallite sizes determined from the width of diffraction peaks are given in Table 1.

Dynamic changes in the electrical resistance, R upon exposure to ammonia, as a function of time, are shown in Fig. 6. The electrical resistance of sensors decreases when ammonia is admitted. Pure TiO_2 sensor is not sensitive enough at 400 °C. The resistivity response to NH_3 of pure SnO_2 nanomaterial is large but irreversible. The composition of 50 mol% SnO_2/50 mol% TiO_2 seems to be stable and sensitive to the interaction with NH_3. The changes in the electrical resistivity are large and reproducible for this nanocomposite sensor.

Figure 7 indicates that the composition of 50 mol% SnO_2/50 mol% TiO_2 gives the highest response to NH_3 at 400 °C. The influence of SnO_2-to-TiO_2 mole ratio of the composite on its response to NH_3 can be explained by a quite complex mechanism of interaction of ammonia with the metal oxide surfaces. There are two types of competitive reactions during oxidation of NH_3 at the sensor surface. One is related to the consumption of the previously chemisorbed oxygen that accounts for normal behavior of adsorption of reducing gases. This reaction leads to a decrease in the sensor resistivity. Inverse reaction with the oxidizing type gas, NO_x which is an oxidation product of NH_3 increases the sensor resistivity. When these two reactions occur at the same time, both

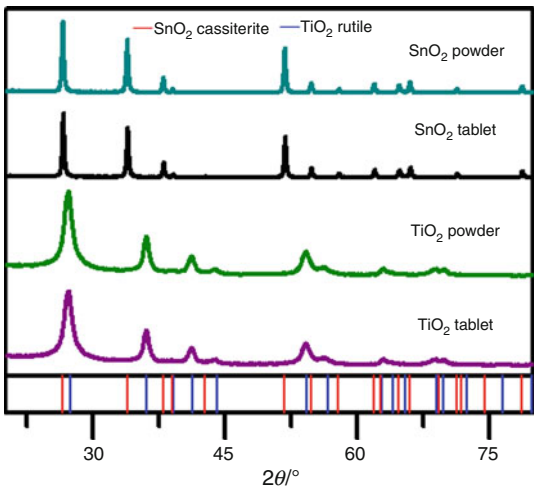

Fig. 4 Comparison of XRD patterns for TiO_2 and SnO_2 nanopowders and gas sensing tablets

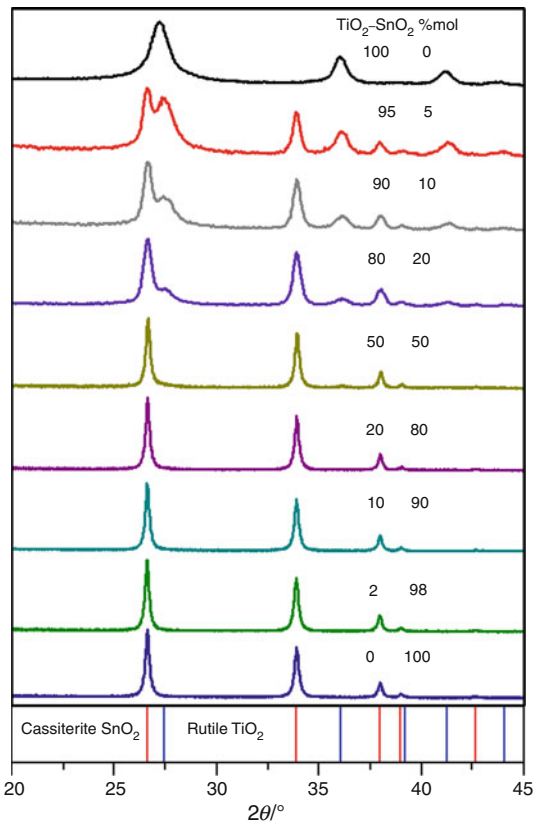

Fig. 5 X-ray diffraction patterns for nanocrystalline TiO_2/SnO_2 composites in the form of gas sensing tablets

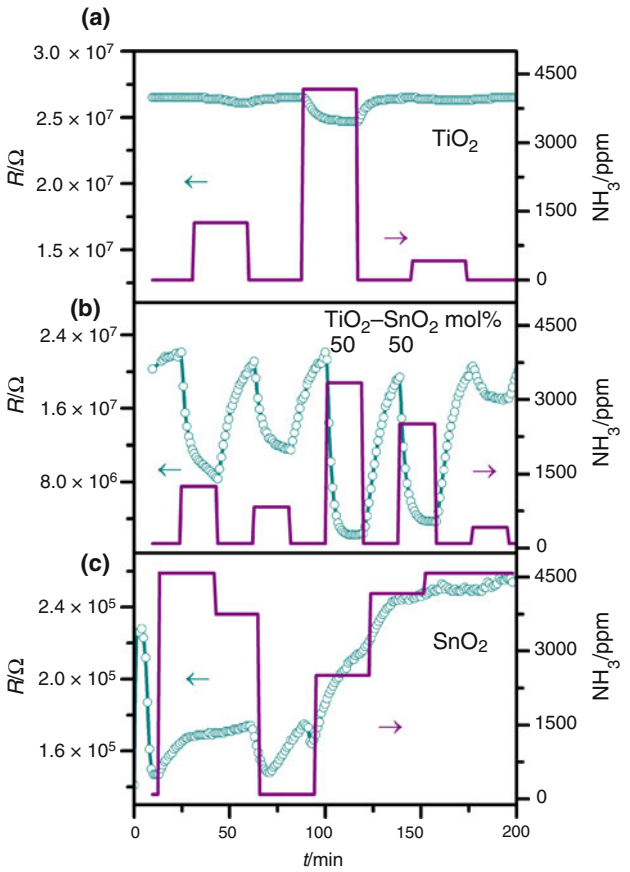

Fig. 6 Changes in the electrical resistance R of gas sensors based on TiO_2, SnO_2 and TiO_2/SnO_2 upon introduction of NH_3 at 400 °C

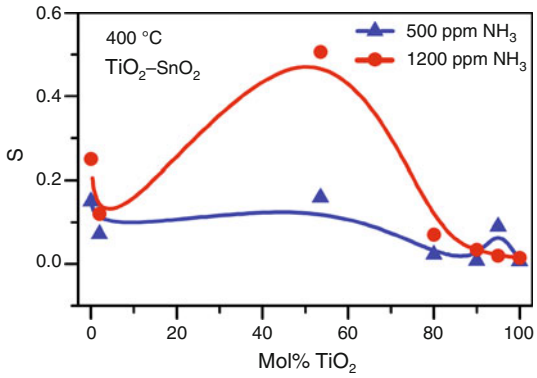

Fig. 7 Gas sensor response, S, as a function of TiO_2/SnO_2 mol ratio at a constant ammonia concentration of 100 ppm and 1200 ppm

effects can cancel out the sensor response. This seems to be the case for pure and TiO_2-rich compounds that are easily affected by both NH_3 and NO_x. SnO_2 is sensitive to NH_3 probably because it is not affected by NO_x. TiO_2 may act as an excellent stabilizer of the resistivity. The presence of grains with different sizes may alter the response through different concentration of the adsorption centers. It seems that the control of the oxidation behavior of NH_3 is important for developing highly sensitive ammonia sensors.

Conclusions

Nanocrystalline TiO_2/SnO_2 composites with chemical compositions varied from 100 mol% TiO_2 to 100 mol% SnO_2 for NH_3 sensing were obtained by mixing pure commercial nanopowders. DTA/TG experiments revealed that thermal decomposition of TiO_2/SnO_2 nanopowders, accompanied by the mass loss and emission of CO_2 and H_2O due to the combustion of organic residue was completed at about 400 °C. This was particularly important for establishing an appropriate calcination temperature of TiO_2/SnO_2 nanocomposites in order to obtain thermally stable NH_3 sensing material. Two separate phases of different crystallite size: smaller rutile TiO_2 and larger cassiterite SnO_2 were revealed by X-ray diffraction. The fact that there were no significant differences in XRD patterns between nanopowders and tablets indicated that the calcination temperature of 400 °C was chosen properly and did not promote the growth of nanoparticles.

The sensor of 50 mol% SnO_2/50 mol% TiO_2 exhibited the best NH_3 sensing features. It was demonstrated that the electrical resistivity of the sensor changed dynamically and reversibly upon interaction with ammonia.

Acknowledgment This work was supported by the Polish Ministry of Science and Higher Education (2009–2012) grant no. N N507 466537.

References

1. Yamazoe N. New approaches for improving semiconductor gas sensors. Sens Actuators B. 1991;5:7–19.
2. Di Francia G, Alfano B, La Ferrara V. Conductometric gas sensors. Hindawi Publishing Corporation, Journal of Sensors, 2009. doi:10.1155/2009/659275.
3. Timmer B, Olthuis W, van den Berg A. Ammonia sensors and their applications—a review. Sens Actuators B. 2005;107:666–77.
4. Ivanov P, Hubalek J, Malysz K, Prášek J, Vilanowa X, Llobet E, Correig X. A route toward more selective and less humidity sensitive screen-printed SnO_2 and WO_3 gas sensitive layers. Sens Actuators B. 2004;100:221–7.
5. Shimizu Y, Okamoto T, Takao Y, Egashira M. Desorption behavior of ammonia from TiO_2-based specimens—ammonia sensing mechanism of double-layer sensors with TiO_2-based catalyst layers. J Mol Catal A Chem. 2000;155:183–91.
6. Zhang W, Zhang W. Fabrication of SnO_2–ZnO nanocomposite sensor for selective sensing of trimethylamine and the freshness of fish. Sens Actuators B. 2008;134:403–8.
7. Yu JH, Choi GM. Electrical and CO gas sensing properties of ZnO–SnO_2 composites. Sens Actuators B. 1998;52:251–6.
8. Khorami HA, Keyanpour-Rad M, Vaezi MR. Synthesis of SnO_2/ZnO composite nanofiber by electrospinning method and study of its ethanol sensing properties. Appl Surf Sci. 2011;257:7988–92.
9. Tang H, Yan M, Zhang H, Li S, Ma X, Wang M, Yang D. A selective NH_3 gas sensor based of Fe_2O_3–ZnO nanocomposites at room temperature. Sens Actuators B. 2006;114:910–5.
10. Kotsikau D, Ivanovskaya M, Orlik D, Falasconi H. Gas-sensitive properties of thin and thick film sensors based on Fe_2O_3–SnO_2 nanocomposites. Sens Actuators B. 2004;101:199–206.
11. Rumyantseva M, Kovalenko V, Gaskov A, Makshina E, Yuschenko V, Ivanova I, Ponzoni A, Faglia G, Comini E. Nanocomposites SnO_2/Fe_2O_3: sensor and catalytic properties. Sens Actuators B. 2006;118:208–14.
12. Shouli B, Dianqing L, Dongmei H, Ruixian L, Aifan C, Liu CC. Preparation, characterization of WO_3–SnO_2 nanocomposites and their sensing properties for NO_2. Sens Actuators B. 2010;150:749–55.
13. Moon WJ, Yu JH, Choi GM. Selective gas detection of SnO_2–TiO_2 gas sensors. J Electron. 2004;13:707–13.
14. Aifan C, Shouli B, Bingjie S, Zhiyong L, Dianging L, Liu CC. Methane gas-sensing and catalytic oxidation activity of SnO_2–In_2O_3 nanocomposites incorporating TiO_2. Sens Actuators B. 2008;135:7–12.
15. Shouli B, Liangyuan C, Pengcheng Y, Ruixian L, Aifan C, Liu CC. Sn/In/Ti nanocomposite sensor for CH_4 detection. Sens Actuators B. 2008;135:1–6.
16. Radecka M, Zakrzewska K, Rekas M. SnO_2–TiO_2 solid solutions for gas sensors. Sens Actuators B. 1998;47:193–9.
17. Carotta MC, Gherardi S, Guidi V, Malagu C, Martinelli G, Vendemiati B, Sacerdoti M, Ghiotti G, Morandi S, Bismuto A, Maddalena P, Setaro A. (Ti, Sn)O_2 binary solid solutions for gas sensing: spectroscopic, optical and transport properties. Sens Actuators B. 2008;130:38–45.
18. Carotta MC, Gherardi S, Guidi V, Malagu C, Martinelli G, Vendemiati B, Sacerdoti M. Electrical and spectroscopic properties of $Ti_{0.2}Sn_{0.8}$ solid solution for gas sensing. Thin Solid Films. 2009;517:6176–83.
19. Zeng W, Liu T, Wang Z. Sensitivity improvement of TiO_2-doped SnO_2 to volatile organic compounds. Phys E. 2010;43:633–8.
20. Zakrzewska K, Radecka M. TiO_2–SnO_2 system for gas sensing—photodegradation of organic contaminants. Thin Solid Films. 2007;515:8332–8.
21. Madarász J, Brăileanu A, Crişan M, Răileanu M, Pokol G. Evolved gas analysis of amorphous precursors for S-doped TiO_2 by TG-FTIR and TG/DTA-MS. J Therm Anal Calorim. 2009;97:265–71.
22. Sergent N, Gélin P, Périer-Camby L, Praliaud H, Thomas G. Study of the interactions between carbon monoxide and high specific surface area tin dioxide. Thermogravimetric analysis and FTIR spectroscopy. J Therm Anal Calorim. 2003;72:1117–26.
23. Pulisova P, Bohacek J, Subrt J, Szatmary L, Bezdicka P, Vecernıkova E, Balek V. Thermal behaviour of titanium dioxide nanoparticles prepared by precipitation from aqueous solutions. J Therm Anal Calorim. 2010;101:607–13.
24. Crisan M, Braileanu A, Crisan D, Raileanu M, Dragan N, Mardare D, Teodorescu V, Ianculescu A, Birjega R, Dumitru M. Thermal behaviour study of some sol-gel TiO_2 based materials. J Therm Anal Calorim. 2008;1:7–13.
25. Banerjee S, Kumar A, Sujatha Devi P. Preparation of nanoparticles of oxides by the citrate-nitrate process. Effect of metal ions on the thermal decomposition characteristics. J Therm Anal Calorim. 2011;104:859–67.
26. http://www.sisweb.com/nist.